A Technique to Localize Activation in the Human Brain with Technetium-99m-HMPAO SPECT: A Validation Study Using Visual Stimulation

Bruce Crosson, David J. G. Williamson, Shailendra S. Shukla, Janice C. Honeyman and Stephen E. Nadeau

Department of Clinical and Health Psychology, College of Health Related Professions, Departments of Neurology and Radiology, College of Medicine, University of Florida, Nuclear Medicine Service, Veterans Affairs Medical Center; and Geriatric Research, Education, and Clinical Center, Veterans Affairs Medical Center, Gainesville, Florida

This study extends and validates a system for localizing brain activity changes based on fiducial markers, coregistration of SPECT and MRI structural images and atlas/MRI-assisted localization. **Methods:** Ten normal subjects underwent ^{99m}Tc-HMPAO SPECT during a resting eyes-closed baseline measurement and during visual stimulation (8-Hz reversing checkerboard). SPECT scans were registered with MRI scans obtained from each individual using a fiducial-based system that minimized z-axis and rotational errors, and registration was further refined along the x- and y-axes by superimposing corresponding axial SPECT and MRI slices. Regions of interest (ROIs) were located on MRI slices with the aid of an atlas. Corresponding loci on SPECT slices were chosen and incrementally adjusted such that the center of a ROI was located precisely at the maximum of activity in the visual cortex or the cortical gray matter ribbon. **Results:** Activity in the calcarine cortex increased by 44.39% during visual stimulation ($p < 0.001$). Adjustment of ROI location in accordance with local activity maxima yielded superior results to a method relying strictly on atlas/MRI localization. Premotor cortex activity declined by 16.91% on the right ($p < 0.01$) and 13.85% on the left ($p > 0.05$), whereas no changes occurred in the somatosensory cortex. **Conclusion:** Changes in visual cortical activity were most comparable to previous functional MRI studies but also congruent with PET and SPECT findings. Using the locus of peak activity to aid in defining cortical ROIs improves the signal-to-noise ratio by reducing noise related to inevitable minor registration errors.

Key Words: SPECT; technetium-99m-HMPAO; regional cerebral blood flow; visual cortex; functional brain imaging

J Nucl Med 1994; 35:755–763

Received Aug. 2, 1993; revision accepted Dec. 20, 1993.

For correspondence or reprints contact: Bruce Crosson, PhD, Department of Clinical and Health Psychology, Box 100165, Health Science Center, University of Florida, Gainesville, FL 32610-0165.

To validate new functional imaging methods for brain activation, it is desirable to use an activation paradigm that has previously produced large and reliable changes in specific brain regions. Studies assessing the effect of visual stimulation on human striate cortex meet this requirement. Several methods have yielded roughly comparable results, including: [^{15}O] water PET to measure regional cerebral blood flow (rCBF) (*1,2*), ^{18}F-fluorodeoxyglucose (^{18}F-FDG) PET to measure regional cerebral glucose metabolism (*3–5*), gadolinium-based MRI to measure regional cerebral blood volume (*6*) and deoxyhemoglobin-based MRI, relying on oxygen extraction differences (*7–9*). Visual stimulation in these studies has consisted of reversing checkerboards (*2,5*), flashing light-emitting diode displays (*1,2,6,8,9*), nonreversing checkerboard patterns (*4*), and a video game (*3*).

Localization procedures for early [^{15}O] water activation studies (*1,2*) involved estimating the position of the anterior commissure-posterior commissure (AC-PC) line from skull landmarks as identified on skull films, maintaining the same head position for PET images as for skull films, mapping PET image planes onto the skull film and translating these planes to a stereotactic atlas referenced to the AC-PC line (*10*). Later studies involving language (*11,12*) extended this technique by standardizing all brains to the same anatomic coordinate system to do intersubject averaging to increase the signal-to-noise ratio.

There are many problems with this technique. First, relatively large s.d.s were reported in validation studies in the localization of an intracranial landmark close to the AC-PC line (the cavernous sinus) (*10*). Localization error is bound to be even higher in most cortical regions, which are much farther from the AC-PC line and more susceptible to rotational errors in image registration. Second, individual subject differences in localization of cortical landmarks, such as the sylvian fissure, after similar standardization may be as high as 1.5 to 2.0 cm (*13,14*), adding a further source of error. Localization of the striate cortex during MRI scanned visual activation confirms suspected variabil-

ity in the anatomic location of this structure (*6*). Third, functional architecture in different individuals does not show an invariant relationship to anatomic landmarks (*14*).

Thus, it is highly desirable to find an alternative region of interest (ROI) localization system that reduces the error inherent in AC-PC-based stereotaxic systems and can take into account individual variations in anatomy. Attempts to map PET images onto MRI images to facilitate anatomic localization have demonstrated some success (*15*), as have studies matching structural and functional MRI images (*6*). One preliminary study of the registration of SPECT and MRI images (*16*) also showed promise. This registration involved the use of three fixed external markers (both ears and glabella) to define a reference plane on both MRI and SPECT. The method was initially validated by measuring errors in the localization of a fourth external marker in SPECT and MRI. Statistical error at points distant from the fiducial markers was comparable to error at the cavernous sinus using AC-PC-based PET (*10*).

SPECT has an advantage over PET in both lower costs and greater availability. The use of ^{99m}Tc-hexamethylpropyleneamine oxime (HMPAO) and SPECT has an advantage over functional MRI in that experiments can be conducted outside the environment of an operating magnet, which presents problems of limited space, high noise level and incompatibility with cathode ray tube-based visual stimulation. However, the only SPECT study of the effect of visual stimulation on the visual cortex is that of Woods et al. (*17*), who used ^{99m}Tc-HMPAO in conjunction with a stroboscopic white light stimulus. These investigators found posterior midline activation comparable to [^{15}O] water PET visual activation studies (*1,2*). Woods et al. also demonstrated a lack of activation in the temporoparietal cortex. However, because the authors could not reference their images to an anatomic atlas, they could not confirm that the observed increases in activity were in the striate cortex, nor could they specify with any degree of precision the location of their temporoparietal values.

We report here the results of our ^{99m}Tc-HMPAO SPECT study of visual activation using a novel ROI localization algorithm. This algorithm uses corresponding MRI slices, an atlas (*18*) and SPECT activation peaks to localize primary visual cortex.

MATERIALS AND METHODS

Subjects

The subjects were 10 men, age range 18 to 27 yr (mean 22.20 yr, s.d. = 2.97), who were recruited through an advertisement in an off-campus student newspaper at the University of Florida. Exclusionary criteria included a history of drug or alcohol abuse and significant head trauma. Subjects were paid for their participation in the study.

Image Acquisition

SPECT images were acquired on a three-headed Triad 88 system (Trionix Research Laboratory, Twinsburg, OH). The within-plane resolution of this camera is 9.3 mm full width-half maximum. Images were acquired with each head rotating 360° in 3° steps, creating 360 raw image sets. In two subjects, technical difficulties with one of the camera heads necessitated using data from only two heads for reconstruction of both stimulated and baseline image sets. The subject's head was positioned in the standard head holder, and he was instructed to remain motionless. Image acquisition required approximately 32 min. T1-weighted MRI images were obtained in axial planes on a Magnetom 1.5-Tesla scanner (Siemens, Iselin, NJ). Slice thickness was 7 mm.

Markers were used to register SPECT and MRI scans in the same image space (*16*). Prior to the experiment, semirigid plastic molds were fashioned from XL-100 Impression System material (JKR Laboratories, Wichita, KS) for both ears and the junction of the nose and the glabella. The distinct impression left on the molds permits reliable placement at precisely the same location on different occasions. Molds were constructed to hold Lucite discs (markers) 25 mm in diameter by 6 mm thick. For SPECT images, a small well in the center of each disk contained 50 μCi of ^{57}Co (Nuclear Associates, Carle Place, NY), which was clearly visible on SPECT images. For MRI scans, the well in each disk contained a 4.5 m*M* copper sulfate solution, which was visible on MRI images.

Procedure

This study was approved by the Institutional Review Board and the Radiation Safety Committee at the University of Florida. Informed consent was obtained from all subjects.

Prior to each SPECT session, an intravenous line containing 0.9% saline solution was placed for injection of the ^{99m}Tc-HMPAO. During both SPECT sessions, the subjects were placed in a quiet room with minimal ambient light. After instructions were given, there was no verbal communication with them until the end of the experimental procedure. They were instructed to sit quietly in an overstuffed chair with their eyes closed for a period of 5 min prior to and 4 min after isotope injection. During this time, the subjects were instructed to try not to picture or verbalize any thoughts and to leave their minds as blank as possible.

Approximately 1 min prior to injection of the isotope, the subjects were tapped on the shoulder, signaling the start of the experiment. For each SPECT scan (baseline and visually activated), 20 or 30 mCi of ^{99m}Tc-HMPAO was injected through the intravenous line. This isotope has a 6-hr half-life. The ligand reaches peak levels within the brain in less than 1 min after injection, and it is extraordinarily stable after reaching 90% of peak value 10 min postinjection (*19*).

In the unactivated baseline session, electroencephalographic monitoring was performed to ascertain the nearly continuous presence of alpha rhythm, thus ensuring that the subjects remained relaxed but awake with eyes closed throughout the session. For the visual stimulation, subjects were seated in the same easy chair with a VM4215 black-and-white television monitor (Sanyo, Bensenville, IL) positioned 125 cm from their eyes. They were instructed to open their eyes and focus on a dot in the center of the monitor screen after their shoulder was tapped. For visual stimulation, a black-and-white reversing checkerboard pattern (similar to that used for visual-evoked potentials) was generated by a Quantum 84 system (Cadwell Laboratories, Kennewick, WA). Stimulus size was 30.5 × 35.6 cm with 18 × 18 mm checks. The repetition rate for reversals was set at 8 Hz because this approximate rate has been found to elicit maximum blood flow changes in the visual cortex (*1,2*). One minute after the subjects opened their eyes, an injection of 20 or 30 mCi of isotope took

place. The subjects watched the reversing checkerboard for 4 min after injection.

Acquisition of SPECT scans commenced at an interval between 20 and 60 min after injection of the isotope. The regional distribution of ^{99m}Tc-HMPAO over this period has been shown to be stable (*19–21*). Given the relatively long half-life (6 hr) of ^{99m}Tc, the relative influence of background noise should change little during this period. Thus, there is no reason to expect that the minor differences in acquisition starting time should significantly affect images or subsequent analyses.

Image Processing and Analysis

Reconstruction and Rotation of Images. SPECT image reconstruction was performed using standard filtered back projection with an attenuation correction factor of 0.12/cm and a 16-point cylindrical algorithm. Image smoothing was accomplished with a Hamming filter (cutoff frequency 0.9/cm). Original images were reconstructed in 64 × 64 pixel axial planes with 3.56 × 3.56 mm pixels and a 3.56-mm slice thickness. After image rotation (discussed later), each two successive SPECT slices were combined to yield a slice thickness of 7.12 mm (negligibly different from the MRI slice thickness of 7.0 mm). MRI images were initially acquired in a 256 × 256 pixel format with 0.90 × 0.90 mm pixels and a 7-mm slice thickness and transferred to the Sun work station accompanying the Triad system. They were then converted to a 128 × 128 pixel format for faster processing (*16*).

Even with careful positioning of the head, the three markers rarely were contained in a single axial plane. However, the software accompanying the Triad-88 camera allowed rotation of the SPECT and MRI scans until the three markers defined a single axial plane. After addition of adjacent slices to obtain a 7.12-mm slice thickness, the three markers could generally be seen on three SPECT slices. Markers generally could be seen on one or two MRI slices. Slices with maximal marker definition were chosen as the reference.

Correction of Pixel Counts. In the brain, ^{99m}Tc-HMPAO becomes trapped when it crosses the blood-brain barrier (BBB) in a lipophilic form and converts to a hydrophilic form that cannot recross the BBB. However, not all the tracer converts to the hydrophilic form immediately on crossing the BBB, and some perfuses back into the blood and is carried away. The level of back perfusion is greater in high-flow areas and requires mathematical correction to make the measured ^{99m}Tc-HMPAO uptake a linear function of rCBF (*19,22*). The equation for this correction is as follows:

$$\text{Corrected } R = \alpha R/(1 + \alpha - R) \qquad \text{Eq. 1}$$

where R is the ratio of counts in the ROI to the counts of some reference region, and α is the conversion to clearance ratio of ^{99m}Tc-HMPAO for the reference region. Each voxel in a SPECT image set was corrected using software incorporating this equation that was written by one of the authors (J.C.H.).

In the literature, both the cerebellum and whole brain have been used as the reference region for the correction equation. Preliminary analyses of uncorrected scans in this study indicated cerebellar activation during visual stimulation in many cases; therefore, whole brain was chosen as the reference region to use in the correction procedure. The true value for α has been shown to be between 1.0 and 2.0 for most brain reference regions (*22*). For the cerebellum, $\alpha = 1.5$ is the accepted value. For whole brain as a reference region, both $\alpha = 1.5$ and $\alpha = 2.0$ produce linear regressions with objective measures of rCBF that approximate a regression line with a slope of +1.0 and an intercept of 0.0 (*19*). We chose to use $\alpha = 2.0$ for two reasons. First, in our subjects, whole-brain flow was almost always noticeably lower than cerebellar flow. Thus, whole brain should have a conversion/clearance ratio higher than the accepted 1.5 for cerebellum. Second, the only other study reporting visual activation imaged by ^{99m}Tc-HMPAO and SPECT (*17*) used $\alpha = 2.0$, and the authors wanted to be able to compare the results found here with those of this other study.

The average whole-brain counts per voxel to use in the correction formula were calculated as follows. The MRI slice above the slice on which the gyrus rectus appears was located. That slice and every third slice above it were selected until a total of four MRI slices were chosen. The outside boundary of the brain on each MRI slice was outlined; Figure 1a shows an MRI slice with the brain outlined in green. Corresponding SPECT slices were selected using the planes identified by the markers as a reference. The SPECT slices were enlarged to 128 × 128 pixels. Each SPECT image was then superimposed on the outline of its respective MRI slice and precisely centered within this outline. Figure 1b shows a SPECT slice aligned with the black outline from the corresponding MRI in Figure 1a. (The white portion of the SPECT image representing brain has been enlarged slightly beyond brain boundaries to make it easier to see the outline from the MRI on the photograph.)

After this alignment, the total counts and numbers of pixels for each slice within the MRI-defined boundary were recorded, and the average counts per voxel for the combined four slices was computed. Preliminary analysis indicated that this value was within 1% to 2% of the average whole-brain count per voxel when all brain slices were included in the calculations. The authors opted to use only every third slice because of the substantial savings in time. This procedure was repeated separately for both stimulated and unstimulated scans to obtain reference values for each. The correction algorithm was then applied to the 64 × 64 pixel SPECT images.

Normalization of Corrected Images. Because there was no significant increase in whole-brain counts with visual activation (Table 1), ROI values were normalized between stimulated and unstimulated scans by equating for whole-brain activity (average counts per voxel), as in previous visual activation studies (*1,2,17*).

Extraction of ROIs. In addition to the striate cortex, two areas from the convexity were chosen for purposes of comparison: primary somatosensory cortex and premotor cortex. For primary somatosensory cortex, a single ROI was taken from the postcentral gyrus (Brodmann's areas 3, 1 and 2). For premotor cortex, two ROIs were taken from Brodmann's areas 6 and 8 and then averaged. In general, striate cortex ROIs were obtained in a manner that maintained some consistency with previous studies (*1,2,6,17*). Because methods developed to sample an area of bilateral activation at the midline were not appropriate to sample lateral ROIs in which changes in activation were not expected on an a priori basis, a different method was developed to sample convexity cortex. Before any ROI extraction, individual SPECT and MRI slices were reregistered, as described earlier under the Correction of Pixel Counts section. This reduced further the modest registration errors associated with complete reliance on our fiducial-based coordinate system (*16*). All ROI extractions were performed on SPECT images that had been enlarged to 256 × 256 (0.89 × 0.89 mm) pixels to minimize errors that can arise with even small misalignments (*23*).

The Damasio and Damasio (*18*) atlas was used to choose ap-

TABLE 1
Percent Activation of Calcarine, Premotor and Somatosensory Regions of Interest and Whole Brain

Subject	Calcarine	Right premotor	Left premotor	Right somatosen	Left somatosen	Whole brain
1	31.55	−21.03	−29.89	8.29	−11.18	−14.85
2	92.37	−17.04	−25.47	1.94	4.24	2.77
3	37.00	−2.19	−1.94	−26.41	−10.25	14.29
4	34.28	−2.11	4.31	9.73	−7.81	−5.16
5	49.35	−19.25	−29.22	−0.74	6.30	6.79
6	79.58	−25.60	−32.09	11.86	−5.49	17.60
7	68.36	−39.68	−39.17	18.97	−8.33	26.47
8	9.26	−9.64	9.08	−22.57	−2.29	26.84
9	11.81	2.90	24.39	6.43	17.78	−8.72
10	30.39	−34.77	−18.52	2.86	4.97	15.70
Mean ± s.d.	44.39 ± 27.80	−16.91 ± 14.21	−13.85 ± 21.30	−1.21 ± 9.31	1.03 ± 14.58	8.12 ± 14.46
t(9)	5.05†	−3.76*	−2.06	−0.41	0.22	1.78

*$p < 0.01$.
†$p < 0.001$.

propriate slices for ROI extraction. The angle of the image slices used consistently corresponded to that of the A-4 plates from this atlas. The atlas section with maximum exposure of striate cortex was selected, and the MRI slice that best matched it was chosen. The corresponding SPECT slice was located by counting the appropriate number of slices from the reference plane defined by the external markers. Previous investigators have noted some intersubject variability in the location of visual cortex along the superoinferior (z-) axis (*6*) and have adjusted slice selection to locate the most active region (*1,2,6,17*). The immediately higher or lower SPECT slice was chosen if, in the activated image, it had visibly greater calcarine activity.

For the first method of calcarine ROI placement (the functional maxima method), a 15 × 30 pixel (13.35 × 26.7 mm) striate cortex ROI was centered along the horizontal (x-) axis at the midline peak of activity. It was located on the anteroposterior (y-) axis to capture the 30 midline pixels with the highest counts in the activated scan. Figure 2a shows the x-axis peak and the y-axis activity at the center of the visual cortex ROI for subject 10. The peak x-axis value and the 30 most active y-axis pixels at this x-coordinate were determined from a pixel by pixel numeric readout of corrected counts. Identical coordinates were used for striate ROIs in unactivated and activated scans. The percentage change in activity was calculated relative to counts in the unactivated scans, as in previous studies (*1,2,6,17*).

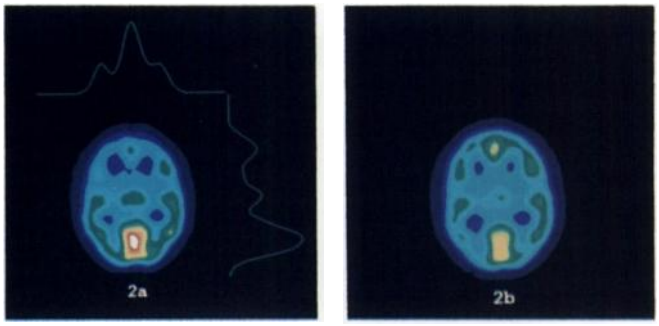

FIGURE 2. (a) Activated visual cortex SPECT image from Subject 10 showing x- and y-axis activity plots, which intersect at the center of the calcarine ROI (as determined by the method of local maxima). (b) Corresponding SPECT image from Subject 10 during unactivated baseline. The activated and unactivated images are on identical 10-point color scales, and the change in visual cortex activity between conditions is readily visible.

This procedure approximates that used in previous studies (*1,2,17*), except for greater constraints on z-axis shifts in this study, and it tends to optimize activation values. However, for a variety of reasons, it cannot be applied to convexity cortex in this experiment. Furthermore, the magnitude of activation seen in

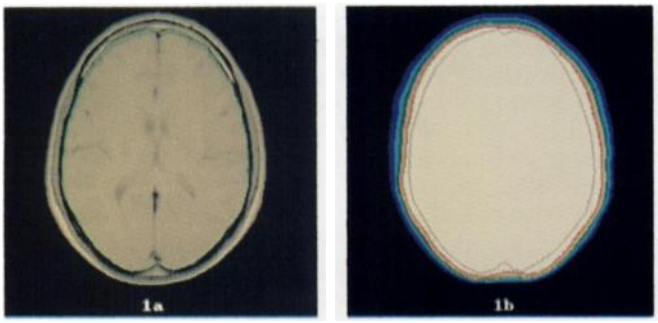

FIGURE 1. (a) MRI at calcarine cortex level for Subject 10 with green outline around brain. (b) Corresponding SPECT image from Subject 10 superimposed and aligned with (black) MRI outline.

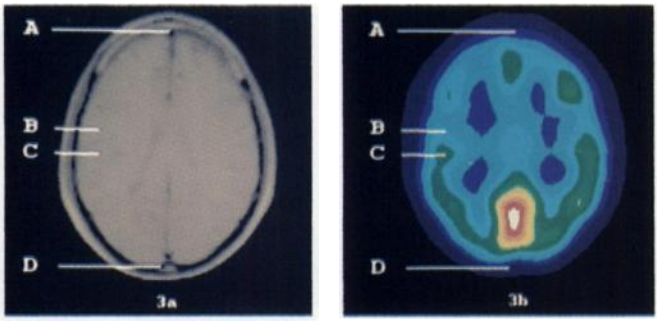

FIGURE 3. (a) Location of somatosensory cortex on MRI as determined from atlas. (b) Location of somatosensory cortex on SPECT as determined from atlas/MRI correspondence.

experiments that examine changes in association cortex is considerably lower than that of striate cortex in visual activation studies (*24*). This lower level of activation makes it impractical to define x-, y- and z-axis loci simultaneously, using local maxima in studies that focus on activity changes in association cortex. Because local maxima cannot be used to define loci on all axes for every occasion, it is desirable to know what magnitude of decrease in activity change would be seen if visual cortex was located using only the atlas and MRI to define ROI location.

Thus, for purposes of comparison, a second method for computing visual cortex activity was used, employing a purely atlas/MRI ROI localization technique. The SPECT slice containing visual cortex was located without allowing the z-axis to vary from the slice dictated by matching the MRI, atlas and SPECT slices (discussed earlier). A 15 × 30 pixel ROI was then centered on the y-axis coordinates dictated by the atlas, similar to the method used for convexity cortex (see following paragraph), and the x-axis center of the ROI was determined by the MRI coordinate of the interhemispheric fissure at the y-axis center of the ROI (Fig. 3).

As just noted, the x- and y-coordinates of ROIs in convexity cortex cannot be precisely defined by SPECT image maxima or MRI landmarks in the same way as calcarine cortex is. Therefore, a different method was used to position convexity ROIs. For the two premotor and primary somatosensory ROIs, the MRI slice corresponding to the seventh slice from the Damasio and Damasio (*18*) atlas was chosen, and corresponding SPECT slices were found. For ROIs oriented less than 45° to the anteroposterior (y-) axis, e.g., somatosensory cortex, the atlas was used to calculate the distance from the anterior margin of the slice to the anterior ROI limit (distance AB on Fig. 4) and the posterior ROI limit (distance AC on Fig. 4) as a proportion of the total length of the slice (distance AD on Fig. 4). The y-coordinate range of the ROI was defined on SPECT/MRI slice coordinates using these same proportions (Fig. 3). Two adjacent 9 × 9 pixel (8.01 × 8.01 mm) squares were centered along the y-axis within this range, and the counts from each square were averaged to obtain a ROI value. The same y-coordinates were used for activated and unactivated scans. Each 9 × 9 pixel square from each ROI was precisely centered along the horizontal (x-) axis at the peak of activity in the cortical gray matter ribbon, as determined from a pixel by pixel readout. For ROIs oriented greater than 45° to the y-axis, e.g., area 8, the same procedure was used, but the axes were reversed (proportional distances were calculated along the x-axis and ROIs were centered on the activity peak along the y-axis). This procedure for ROI localization and positioning was chosen because early experience showed that small errors in SPECT-MRI image registration were unavoidable, and yet an error of as little as a single acquisition pixel in size (3.56 mm) could result in changes in measured activity of as much as 20%. Other investigators have reported similar findings (*23*).

RESULTS

The percent change for each subject in the striate cortex, premotor and somatosensory ROIs is displayed in Table 1. A positive change denotes relatively greater activity on the stimulated SPECT scan, whereas a negative change denotes relatively greater activity on the unstimulated scan. Two-tailed t-tests were calculated for changes in each ROI, comparing the observed change to a null hypothesis of zero change. The resulting t-values are displayed at the bottom of each column in Table 1.

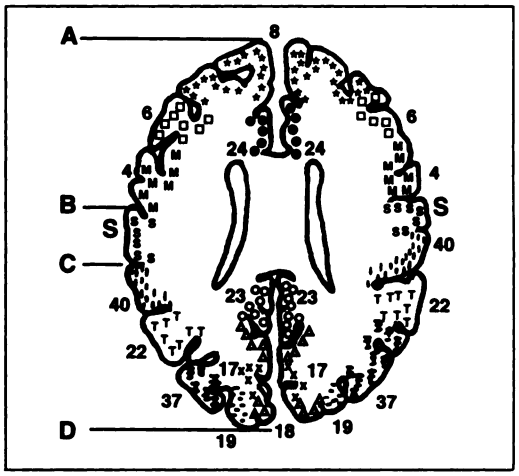

FIGURE 4. Boundaries of somatosensory ROI and anterior and posterior extent of brain on atlas slice used to determine proportional distances. Proportional distances (AB/AD and AC/AD) are then used to define the somatosensory ROI on MRI, and subsequently SPECT (Fig. 3) (*18*). (Reprinted with permission from Damasio H, Damasio AR: *Lesion analysis in neuropsychology*. New York: Oxford University Press, 1989.)

Every subject demonstrated increased activity in the striate cortex during visual stimulation, although the magnitude of change varied considerably between subjects. The mean change (44.39%) was highly significant ($p < 0.001$). Figure 2 shows identically scaled activated (Fig. 2a) and baseline (Fig. 2b) images in the visual cortex slice for subject 10. There were no significant changes in activity for the right or left somatosensory ROIs. There was a reduction in activity in both premotor areas during visual stimulation, but this decrease was statistically significant only on the right ($p < 0.01$). Although this finding was unexpected, it was consistent with findings from some previous studies (see Discussion).

Results of the atlas/MRI-based calcarine ROI placement scheme are shown in Table 2. The resulting increase in visual activity with visual stimulation was still significant ($t(9) = 4.06$, $p < 0.01$). The results achieved with this method of ROI placement and the local maxima method were fairly comparable ($r = 0.90$, $p < 0.0005$), but the average change with the atlas/MRI method was only 80% of the change with the local maxima method, a reduction by approximately 1 s.e.m. Thus, some sensitivity was lost with the atlas/MRI method.

The variability in visual activation also was larger than expected. Several possible reasons for this were explored. One such possibility was that the angle of the image slices was different from that of previous studies. Rotating the glabella marker into registration with the ear markers produces relatively steep cuts, approximately 15° with respect to the AC-PC line. To ascertain whether this angle was responsible for the greater-than-expected variability, uncorrected images were rotated −15° to more nearly approximate the angle of the AC-PC line. Images were then corrected to be linear with blood flow, and striate cortex ROIs were extracted as described earlier (i.e., using the local

TABLE 2
Percent Change Using Different Methods of Calculating Calcarine Region of Interest Activity

Subject	No rotation local maxima*	No rotation atlas/MRI†	−15° Rotation local maxima‡	Different method§
1	31.55	14.68	28.06	17.19
2	92.37	62.60	93.45	39.37
3	37.00	24.32	34.84	23.64
4	34.28	6.57	8.32	22.25
5	49.35	53.52	47.11	34.73
6	79.58	79.10	79.28	50.39
7	68.36	69.84	70.97	45.61
8	9.26	6.49	16.30	12.60
9	11.81	13.47	13.60	9.25
10	30.39	26.49	32.20	25.73
Mean ± s.d.	44.39 ± 27.80	35.71 ± 27.77	42.41 ± 29.52	25.82 ± 12.68

*Calcarine region of interest located using local maxima on x-, y- and z-axes (see text).
†Calcarine region of interest located strictly in accordance with atlas and MRI criteria on x-, y- and z-axes, i.e., no shifts allowed for local maxima (see text).
‡Equivalent to Damasio and Damasio (*18*) A-2 slices; parallel to anterior commissure-posterior commissure line. Region of interest localization performed using local maxima on x-, y- and z-axes.
§Scans were corrected using cerebellum as the reference region and $\alpha = 1.5$; location of calcarine region of interest performed by different operator (see text).

maxima method), except the A-2 plates from the Damasio and Damasio (*18*) atlas were used. The results for each subject are shown in Table 2. It can be seen that, with one exception, the correspondence between the results of the two methods is high. In fact, the product-moment correlation between the two sets of findings was 0.95 ($p < 0.0001$).

Other factors, such as the individual operator extracting ROIs, the method for extracting ROIs, the conversion/clearance ratio used to correct images and the reference region used in the correction process could have contributed to the variance. Therefore values were compared from the original analysis with values from images extracted by a different operator, using a different method for extracting ROIs, on different size SPECT images (128 × 128 pixels), with a smaller conversion to clearance ratio ($\alpha = 1.5$, as originally recommended by Lassen et al. (*22*)) using a cerebellar reference region. The method of striate ROI extraction involved finding a 5 × 10 pixel ROI at the center of the striate activation region on a 128 × 128 pixel image in a manner similar to the method described earlier but with two differences. First, the choice of SPECT slice was not allowed to vary on the z-axis. Second, the ROI on the unstimulated scan was centered on the most active 5 × 10 (1.78-mm) pixel region along the midline calcarine peak, rather than at the same y-coordinate as in the activated scan. These findings are also presented for each subject in Table 2. The correlation between the latter method and the local maxima method is high ($r = 0.92$, $p < 0.0001$). Thus, it seems unlikely that angle of slice, individual operator differences, method of ROI extraction, the size to which SPECT images were enlarged or the reference region used for correction of images made substantial differences, although the ratio of the mean to the s.e.m. was slightly less for the alternate method just described, as was the mean change in striate activity.

DISCUSSION

A simple algorithm was described for calculating activity changes in striate and nonstriate cortex based on a modification of a fiducial-based SPECT-MRI registration system referenced to a widely available atlas. This algorithm was tested in a visual activation paradigm. Previous findings (*6*) indicated that the location of primary visual cortex is somewhat variable and more dorsal in some individuals than in others. Accordingly, the SPECT slice was chosen immediately above or below that indicated by correlation of the MRI and atlas if visibly greater activity was apparent in this slice on the activated SPECT scan. Furthermore, some variation in the anteroposterior and lateral location of local maxima exists (*6*); for this reason, a method of local maxima was used to center a ROI within this slice on the cortex that was most active during visual stimulation. Although a method relying totally on atlas and MRI localization also produced significant results, there was some drop in efficiency (i.e., a decreased ratio of the mean to the s.e.m.). Such a loss in efficiency is acceptable under conditions of favorable signal/noise ratio, but the ability to recognize true changes could be compromised as the signal/noise ratio falls. This problem in atlas-driven methods has been recognized by previous investigators (*14*).

Thus, it would be desirable to have a more precise registration between the actual location of the calcarine sulcus on MRI and activity changes on the SPECT scan. Such precision was not possible using the axial MRI images acquired for the current study, but it might be possible to use sagittal MRI and SPECT images. Sagittal MRI reconstructions of sufficient quality could not be produced to carry out this analysis, but this is a technical limitation that can be overcome.

TABLE 3
Means, Standard Deviations and Ranges of Change in Calcarine Activity (in Percent) in Visual Activation Studies

Study	Stimulus	Method (FWHM resolution)	Mean	s.d.	Range
Fox et al. (*1*)	7.8-Hz LED patterned flash	[^{15}O] water PET rCBF (11.7 mm)	31.46	6.22	21.49–42.45
Goffinet et al. (*3*)	Video Game	^{18}F-FDG rCM (8–9 mm)	16.5	7.3	7.2–33.6
Belliveau et al. (*6*)	7.8-Hz LED patterned flash	Gadolinium MRI rCBF* (–)	58.0	22.1	35.9–92.5
Woods et al. (*17*)	10-Hz stroboscopic flash	^{99m}Tc-HMPAO SPECT (?)	36.7	6.6	28.7–44.3
Current study	8-Hz reversing checkerboard	^{99m}Tc-HMPAO (9.3 mm)	44.39	27.80	9.26–92.37

*To compare Belliveau et al.'s (1991) figures to rCBF changes from other studies, regional cerebral blood volume (plasma) changes were converted to regional cerebral blood volume (hematocrit) changes and then to rCBF, using formulae given by Sakai et al. (*25*) and Grubb et al. (*26*), respectively.

LED = light-emitting diode; rCBF = regional cerebral blood flow; FDG = fluorodeoxyglucose; HMPAO = hexamethylpropyleneamine oxime.

The variability between subjects was larger than anticipated from some previous studies (*1,2,17*). Four other visual stimulation studies in the literature gave individual subject values for calcarine activity that could be converted to percent changes as in this study. The mean striate cortex activation, s.d. and range for each study are shown in Table 3. Three studies, including the present one, were rCBF studies. For purposes of comparison, one study (*6*) was converted from regional cerebral blood volume to rCBF (see Table 3 footnote). One ^{18}F-FDG study could not be converted to rCBF.

Although the standard deviation in the current study is greater than that of Fox et al. (*1*) or Woods et al. (*17*), it is only slightly greater than that of Belliveau et al. (*6*). Although the absolute values of glucose metabolism change (*3*) cannot be compared with rCBF values, the ratio of the mean to the s.d. in that study was more nearly comparable to that of Belliveau et al. (*6*) than it is to that of Fox et al. (*1*) or Woods et al. (*17*).

Thus, there is considerable variation in the s.d. of calcarine activation in reported studies. This variation does not seem to be a product of differing image resolution because image resolution was comparable in these studies. Nor does the variation seem to be a product of temporal resolution. The techniques with greater temporal resolution (MRI (*6*) and [^{15}O] water rCBF (*1,2*)) showed a large difference in variability. This study and that of Woods et al. (*17*) used the same isotope and should have similar temporal resolution.

One difference between studies that may be important in accounting for differential intersubject variability is the use of MRI and atlas-guided localization. This study and that of Belliveau et al. (*6*), both of which used such techniques, were characterized by relatively higher s.d. Woods et al. (*17*) chose the one slice of five that showed the highest percent change. Their lowest slice was near or slightly above the level of the basal ganglia, and the center of their highest slice was 2.4 cm above the center of their lowest slice (6-mm slice thickness). A review of coronal plates of a detailed atlas (*27*) indicates that Woods et al.'s highest slice could have been sampling mesial limbic or parietal cortex in part, including mesial area 7. Mesial area 7 was sampled in these subjects (approximately 2.1 cm above striate cortex). There was significant activation of this cortex, and in two cases, mesial area 7 activation exceeded that of striate cortex. One of these two cases showed the lowest percent activation of striate cortex, and the mesial area 7 activation exceeded that of striate cortex substantially, 23.91% versus 9.26%, respectively. The authors detail this extrastriate activation in a separate article, which is currently in preparation. Fox et al. (*1*) claimed that their areas of peak activation were located in striate cortex, but they offered no data to back up this claim. They also used a slice thickness twice that of the current study. Such an increase in slice thickness would have the effect of reducing higher activation values by averaging highly activated cortex with less activated cortex or of striate cortex activity with nonstriate cortex activity.

Another possible explanation for the higher striate activation variability in the current study is the nature of the visual stimulation. The stroboscopic flash used by Woods et al. (*17*) was a brighter stimulus than the reversing checkerboard used here. The goggles used by Belliveau et al. (*6*) and Fox et al. (*1,2*) may have more efficiently precluded outside stimulation. Indeed, this may be the reason why two of the subjects here fell below the range of values seen in the Belliveau et al. (*6*) study; otherwise, the values in the two studies are similar. Finally, behavioral paradigms could have played a role in differences between studies. The authors attempted to isolate the subjects from internal and external stimulation for a period of 5 min prior to visual stimulation. Similar procedures have not been reported in other studies. Variable responses during this 5-min period may have led to some subsequent variation in baseline responses.

The use of cerebellar values to correct images in the current study yielded a slightly more favorable relationship between the mean and s.e.m. than did using whole-brain values. This relative reduction in the s.e.m. occurred primarily because subjects with greater striate cortex activation demonstrated lower percent activation scores using a cerebellar than a whole-brain reference region. However, preliminary analyses indicated that there was a significant

activation of cerebellum during visual stimulation, whereas such a difference did not occur for whole-brain values. For this reason, whole brain was chosen as the reference.

It seems unlikely that having subjects close their eyes during the baseline condition would have contributed either to the magnitude or variability in visual activation. Because Woods et al. (*17*) patched the eyes of their subjects during their baseline state and their subjects' eyes presumably were closed, eye closure cannot be the source of different findings between that study and this. Although one previous study (*5*) compared eyes-open and eyes-closed conditions, the subjects were looking at white light in the eyes-open condition and thereby receiving visual stimulation. Changes in functional images associated purely with eye closure (i.e., using an eyes-open reduced-lighting condition for comparison) have not been performed. Nonetheless, eye closure induces increased alpha activity, and the authors cannot absolutely rule out significant effects related to eye closure on the basis of our findings or previous findings (*5,17*).

The mean change in calcarine activity in this study was greater than in the other ^{99m}Tc-HMPAO SPECT study, comparable to [^{15}O] water PET and ^{18}F-FDG PET studies and approached that of the functional MRI study of Belliveau et al. (*6*) (Table 3). The authors believe this higher value reflects greater precision in localization of the calcarine ROI and hence less volume averaging with less activated tissue. Functional MRI is likely to achieve optimal precision in calcarine ROI location, the least volume averaging with less active tissue and the maximal measures of changes in calcarine activity. The report by Belliveau et al. (*6*) supports this hypothesis.

Finally, the deactivation of premotor cortex during visual stimulation should be briefly addressed. This decrease in activity was found to extend to the dorsolateral frontal and anterior cingulate cortex; these findings are discussed in a separate article. Similar findings have never been reported with [^{15}O] water rCBF (*1,2,28*). However, deactivation of various frontal areas has been reported with ^{18}F-FDG studies while comparing monitoring of a checkerboard stimulus with simple visual fixation (*4*), watching a video game with an eyes-closed rest state (*3*) and normal controls with patients having severe bilateral optic neuropathy (*29*).

In summary, these findings suggest that ^{99m}Tc-HMPAO SPECT, in conjunction with a modified fiducial-based MRI registration system and an atlas, can be used to assess the activation of striate and nonstriate cortex in a manner that may overcome some of the difficulties and limitations inherent in other functional imaging methods. The findings in a visual activation paradigm were comparable to those of some previous studies, although the variability was higher. The greater variability is probably caused by a combination of factors, including the localization method, slice thickness and stimulation method. Future studies could help resolve the localization issue by using sagittal MRI images to locate the appropriate cortex and sagittal SPECT images to test activation at that location. Activation of association cortex can be expected to be of lower magnitude than activation of striate cortex (*24*). In such circumstances, the drop in efficiency noted with a purely atlas/MRI-based ROI placement scheme becomes more critical and may jeopardize the ability to recognize true activity changes. Therefore, in studies of association cortex activation, maximum accuracy in anatomic localization for each individual subject is desirable (*14*). The use of sagittal MRI and SPECT images, or better yet, three-dimensional reconstructions would allow a greater use of sulcal anatomy to specify ROIs in many instances, thereby increasing the accuracy of localization for individual subjects. Some attempts also should be made to cross validate ^{99m}Tc-HMPAO SPECT, ^{18}F-FDG PET, [^{15}O] water PET and functional MRI techniques to determine the strengths and weaknesses of each technique. The perfection of more cost-effective technologies, such as ^{99m}Tc-HMPAO SPECT and functional MRI, could lead to great advances in understanding normal brain functions.

ACKNOWLEDGMENTS

The authors thank Clyde M. Williams, MD, PhD, without whose administrative and conceptual support this study would have been impossible. The authors also thank Morris Thompson who performed all injections of isotope and SPECT acquisitions for this study. This project was supported through a Research Support for New Faculty Program award from the University of Florida Division of Sponsored Research.

REFERENCES

1. Fox PT, Raichle ME. Stimulus rate dependence of regional cerebral blood flow in human striate cortex, demonstrated by positron emission tomography. *J Neurophysiol* 1984;51:1109–1120.
2. Fox PT, Raichle ME. Stimulus rate determines regional brain blood flow in striate cortex. *Ann Neurol* 1985;17:303–305.
3. Goffinet AM, DeVolder AG, Bol A, et al. Brain glucose utilization under high sensory activation: hypoactivation of prefrontal cortex. *Aviat Space Environ Med* 1990;61:338–342.
4. Kushner MJ, Rosenquist A, Alavi A, et al. Cerebral metabolism and patterned visual stimulation: a positron emission tomographic study of the human visual cortex. *Neurology* 1988;38:89–95.
5. Phelps ME, Mazziotta JC, Kuhl DE, et al. Tomographic mapping of human cerebral metabolism: visual stimulation and deprivation. *Neurology* 1981; 31:517–529.
6. Belliveau JW, Kennedy DN, McKinstry RC, et al. Functional mapping of the human visual cortex by magnetic resonance imaging. *Science* 1991;254: 716–719.
7. Kwong KK, Belliveau JW, Chesler DA, et al. Real time imaging of perfusion change and blood oxygenation change with EPI. *Proceedings for the Society for Magnetic Resonance in Medicine annual meeting*. Baltimore: Williams and Wilkins; 1992:301.
8. Ogawa S, Tank DW, Menon R, et al. Functional brain mapping using MRI: intrinsic signal changes accompanying sensory stimulation. *Proceedings for the Society for Magnetic Resonance in Medicine annual meeting*. Baltimore: Williams and Wilkins; 1992:303.
9. Turner R, Jezzard P, Wen H, et al. Functional mapping of the human visual cortex at 4 Tesla using deoxygenation contrast EPI. *Proceedings for the Society for Magnetic Resonance in Medicine annual meeting*. Baltimore: Williams and Wilkins; 1992:303.
10. Fox PT, Perlmutter JS, Raichle ME. A stereotactic method of anatomical localization for positron emission tomography. *J Comput Assist Tomogr* 1985;9:141–153.
11. Petersen SE, Fox PT, Posner MI, et al. Positron emission tomographic studies of cortical anatomy of single-word processing. *Nature* 1988;331:585–589.

12. Petersen SE, Fox PT, Snyder AZ, et al. Activation of extrastriate and frontal cortical areas by visual words and word-like stimuli. *Science* 1990; 249:1041–1044.
13. Steinmetz H, Furst G, Fruend H-J. Variation of perisylvian and calcarine anatomic landmarks within stereotaxic proportional coordinates. *Am J Neuroradiol* 1990;11:1123–1130.
14. Steinmetz H, Seitz RJ. Functional anatomy of language processing: neuroimaging and the problem of individual variability. *Neuropsychologia* 1991;29:1149–1161.
15. Mora BN, Carmen GJ, Allman JM. In vivo functional localization of the human visual cortex using positron emission tomography and magnetic resonance imaging. *Trends Neurosci* 1989;12:282–284.
16. Shukla SS, Honeyman JC, Crosson B, et al. Method for registering brain SPECT and MR images. *J Comput Assist Tomogr* 1992;16:966–970.
17. Woods SM, Hegeman IM, Zubal IG, et al. Visual stimulation increases technetium-99m-HMPAO distribution in human visual cortex. *J Nucl Med* 1991;32:210–215.
18. Damasio H, Damasio AR. *Lesion analysis in neuropsychology.* New York: Oxford University Press; 1989.
19. Andersen AR, Friberg HH, Schmidt JF, et al. Quantitative measurements of cerebral blood flow using SPECT and [99mTc]-d,l-HM-PAO compared to xenon-133. *J Cereb Blood Flow Metab* 1988;8:S69–S81.
20. Leonard J-P, Nowotnik DP, Neirinckx RD. Technetium-99m-d,l-HM-PAO: a new radiopharmaceutical for imaging regional brain perfusion using SPECT—a comparison with iodine-123 HIPDM. *J Nucl Med* 1986;27:1819–1823.
21. Neirinckx RD, Canning LR, Piper IM, et al. Technetium-99m-d,l-HM-PAO: a new radiopharmaceutical for SPECT imaging of regional cerebral blood perfusion. *J Nucl Med* 1987;28:191–202.
22. Lassen NA, Andersen AR, Friberg L, et al. The retention of [99mTc]-d,l-HM-PAO in the human brain after intracarotid bolus injection: a kinetic analysis. *J Cereb Blood Flow Metab* 1988;8:S13–S22.
23. Phillips RL, London ED, Links JM, et al. Program for PET image alignment: effects on calculated differences in cerebral metabolic rates for glucose. *J Nucl Med* 1990;31:2052–2057.
24. Raichle ME. Memory mechanisms in the processing of words and word-like symbols. In: Chadwick DJ, Whelan J, eds. *Exploring brain anatomy with positron tomography (Ciba Foundation Symposium 163).* New York: John Wiley & Sons; 1991:198.
25. Sakai F, Nakazawa K, Tasaki Y, et al. Regional cerebral blood volume and hematocrit measured in normal human volunteers by single-photon emission computed tomography. *J Cereb Blood Flow Metab* 1985;5:207–213.
26. Grubb RL, Raichle ME, Eichling JO, Ter-Pogossian MM. The effects of changes in $Paco_2$ on cerebral blood volume, blood flow, and vascular mean transit time. *Stroke* 1974;5:630–639.
27. Talairach J, Tournoux P. *Co-planar stereotaxic atlas of the human brain.* New York: Thieme Medical Publishers; 1988.
28. Fox PT, Miezin FM, Allman JM, et al. Retinotopic organization of human visual cortex mapped with positron-emission tomography. *J Neurosci* 1987; 7:913–922.
29. Kiyosawa M, Bosley TM, Kushner M, et al. Positron emission tomography to study the effect of eye closure and optic nerve damage on human cerebral glucose metabolism. *Am J Ophthalmol* 1989;108:147–152.